Isotope effects on energy, particle transport and turbulence in electron cyclotron resonant heating plasma of the Large Helical Device

Isotope effects on energy, particle transports and turbulence in ECRH plasma of LHD

K. Tanaka[1,2], Y. Ohtani[3], M. Nakata[1,4], F. Warmer[5], T. Tsujimura[1], Y. Takemura[1,4], T. Kinoshita[2], H. Takahashi[1,4], M. Yokoyama[1,4], R. Seki[1,4], H. Igami[1], Y. Yoshimura[1], S. Kubo[1], T. Shimozuma[1], T. Tokuzawa[1], T. Akiyama[6], I. Yamada[1], R. Yasuhara[1,4], H. Funaba[1], M. Yoshinuma[1], K. Ida[1], M. Goto[1,4], G. Motojima[1,4], M. Shoji[1], S.Masuzaki[1], C.A. Michael[7], L.N. Vacheslavov[8,9], M. Osakabe[1,4], T. Morisaki[1,4]

[1] National Institute for Fusion Science, National Institutes of Natural Sciences, Toki, Gifu, 509-5292, Japan
[2] Kyushu University, Department of Advanced Energy Engineering, Kasuga, Fukuoka, 816-8580, Japan
[3] National Institutes for Quantum and Radiological Science and Technology, Naka, Japan
[4] SOKENDAI (The Graduate University for Advanced Studies), Toki, Gifu, 509-5292, Japan
[5] Max-Planck-Institut für Plasmaphysik, Greifswald, Germany
[6] General Atomics, San Diego, California, USA
[7] University of California-Los Angeles, Los Angeles, California, USA
[8] Budker Institute of Nuclear Physics, 630090 Novosibirsk, Russian Federation
[9] Novosibirsk State University, Novosibirsk 630090, Russian Federation

E-mail contact of main author: ktanaka@nifs.ac.jp

Abstract

The positive isotope effects have been found in ECRH plasma of LHD. The global energy confinement time (τ_E) in deuterium (D) plasma is 16% better than in hydrogen (H) plasma for the same line averaged density and absorption power. The power balance analyses showed that clear reduction of ion energy transport, while electron energy transport does not change dramatically. The global particle confinement time (τ_p) is degraded in D plasma. τ_p in D plasma is 20% worse than in H plasma for same line averaged density and absorption power. The difference of the density profile was not due to the neutral or impurity sources, but rather was due to the difference of the transport. Ion scale turbulence levels show isotope effects. The core turbulence (ρ = 0.5 - 0.8) level is higher in D plasma than in H plasma in low collisionality regime and is lower in D plasma than in H plasma. Density gradient and collisionality play a role in core turbulence level.

1. INTRODUCTION

The transport of different hydrogen isotopes is an important issue for predicting the performance of ITER and the future reactor operation. In a tokamak, improved transport character and lower H mode threshold power in D plasma than in H plasma were reported. Both tokamak scaling (ITER98y2[1]) and helical scaling (ISS04[2]) follow gyro-Bohm (GB) scaling. GB scaling predicts that global energy confinement time scale with $A^{0.5}$, where A is ion mass number (1 for H, 2 for D) , then GB scaling enhanced transport in D plasma. However, many experiments show better confinement (in tokamak) in D or comparable confinement (in medium-sized helical devices).

In JET with ITER-like wall, τ_E scales with $A^{0.15}$, in L mode and τ_E scales with $A^{0.4}$ in H mode[3]. In JT-60U tokamak, clear improvements of ion thermal confinement were observed. Only one half of the heating power was necessary in D plasma compared with heating power in H plasma to obtain the identical density and temperature profiles in neutral beam (NB) heated H mode with carbon wall. The higher edge pedestal improved core confinement due to the ion temperature stiffness [4]. In ASDEX-U electron cyclotron resonant heating (ECRH) L mode plasma, τ_E scales with $A^{0.2}$. The results show that the better τ_E in D plasma than in H plasma is not due to the improvement of the transport, but is due to the difference of

equipartition heating (P_{ei}) from electron to the ion. Higher P_{ei} in H plasma results in degraded τ_E due to the power degradation [5]. These results in tokamak suggest that confinement improvements in D plasma mainly come from edge pedestal.

On the other hand, the result of the hydrogen isotope effects are very limited in stellarator/heliotron. In the early study of medium size stellarator/heliotron (Heliotron-E, ATF, W-7AS), the global energy confinement time of ECRH plasma was almost comparable. The scaling study showed the modest improvement in D plasma compared to that in H plasma, but, the difference is within the uncertainty [6]. In NB heated plasma of CHS, τ_E was worse in D plasma than in H plasma in low collisionality regime, and global confinement time (τ_p) was comparable. However, density modulation experiments showed lower diffusion, and more inwardly directed convection velocity in low density regime were reported [7]. In Heliotron-J, density modulation experiments were performed in D and H plasma with ECRH. Comparable diffusion coefficients and convection velocities were reported [8]. In stellarator/heliotron, due to the limit of the datasets, a comprehensive picture of the isotope effects is not yet obtained.

In LHD, the deuterium experimental campaign started from March 2017 [9]. This paper treats pure ECRH plasma, which are free from beam heating effects and presents the survey of particle transport in addition to energy transport. Initial reports regarding ECRH plasma were published in refs. 10 and 11. These results describe improvement in high power heating ECRH [10], scaling study and comparison with neoclassical transport [11] with assistance of NB heating. In ref. 2, the datasets of ECRH plasma includes different injection direction of tangential ECRH. The tangential ECRH induces ECCD and affects iota profiles. This can affect transport also can stochasticity [10, 12]. Thus, in order to investigate the isotope effects, the injection direction was mainly a balanced injection in order to prevent the change of the iota profile and formation of stochastic region. ECRH is possible to adjust the total deposition power in H and D plasma, although in NBI, it is not technically easy. Thus, clear and simple comparison became possible from the dataset analysed in this publication.

2. ENERGY TRANSPORT

Figure 1 shows summary of global energy (τ_E). τ_E was estimated from diamagnetic stored energy and power deposition calculated by LHDGAUSS [13]. In the dataset, the contamination of helium was less than 10% and the purity of the H and the D were higher than 80%, respectively. In the dataset, the injection power was 0.6-3.9MW in D, 0.8-3.8MW in H, the line averaged density ($n_{e\ bar}$) was 0.6-2.8x10^{19}m^{-3} in D, and was 0.3-2.8x10^{19}m^{-3} in H. The one path absorption power was 91+-3% in D 93+-3% in H plasma. Only one path absorption power was used for the τ_E estimation. The magnetic axis position (R_{ax}) was 3.6m and magnetic field strength at magnetic axis (Bt) was 2.75T. The magnetic axis position at R_{ax}=3.6m are most widely operated in LHD. This is because confinement was the best compared with other outer shifted configurations [2].

The normalized collisionality ν^*_h is defined as $\nu^*_h = \nu_{ei}/(\varepsilon_{eff}^{3/2}\nu_T/qR_{mj})$. ν_{ei} is the electron ion collision frequency, ν_T is the electron thermal velocity, q is the safety factor, R_{mj} is the major radius, and ε_{eff} is an effective helical ripple [14, 15]. The total collision frequency is the sum of ν_{ei} and ν_{ii} (ion-ion collision frequency). For H or D ion, ν_{ei} is approximately one order magnitude larger than ν_{ii} in ECRH plasma, thus, ν_{ei} is used as a representative value.

ν^*_h =1 corresponds to the boundary of 1/ν and plateau regime in helical/stellarator [16], which corresponds to approximately banana regime and plateau regime in tokamak with the same aspect ratio of LHD. The ν_h^* at ρ = 0.5 was used as a representative value.

As shown in Fig.1 (a), τ_E is systematically higher in D. This is more apparent in the high collisionality regime. The improvement in D appears at $\nu_h^* \sim>1$. As shown in Fig.1 (b), the

hydrogen data sets almost follow ISS04 [2] scaling, while deuterium dataset is systematically higher than ISS04 prediction. The averaged enhancement factors are $\tau_E / \tau_{E\,ISS04}$=1.19+-0.11 in D and 1.04+-0.15 in H plasma. However, as shown in Fig. 1 (c), the enhancement factor depends on ν_h^*. The enhancement factor has a maximum at $\nu_h^* \sim 1.5$ both in H and D plasma. Finally, the scaling was deduced from the dataset of the 2017 campaign.

$$\tau_{E\,dia.ECH} \propto A^{0.22\pm0.01} \bar{n}_e{}^{0.60\pm0.01} P_{abs}^{-0.51\pm0.01} \quad (1)$$

Here, A is mass number (1 for H plasma, 2 for D plasma), $\bar{n}_e$ is the line averaged density, and P_{abs} is the absorption power. For same $\bar{n}_e$ and P_{abs}, τ_E in D plasma is 16% better than in H plasma.

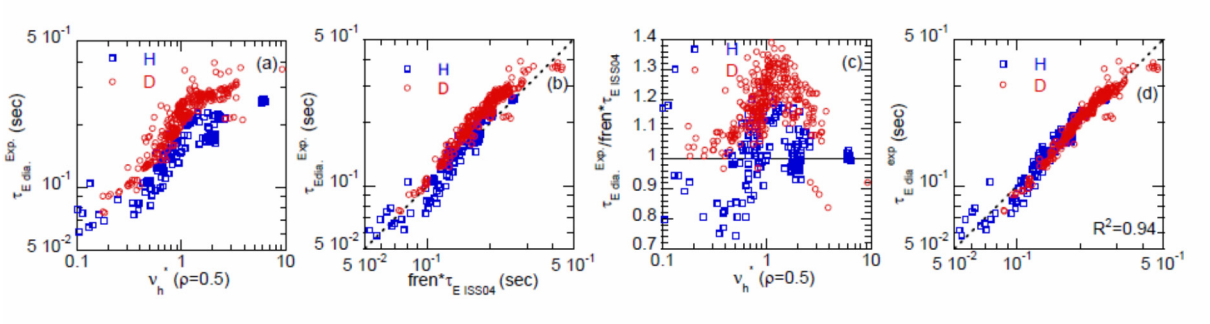

FIG. 1. τ_E of (a) collisionality dependence, (b) comparison with ISS04 scaling, (c) collisionality dependence of enhancement factor and (d) deduced scaling from the 2017 19th experimental campaign. In Fig.1 (b), fren is the normalization factor of ISS04 and is 0.93 for R_{ax}=3.6m [2].

Local power balance analysis was carried out by using TASK3D code [17] for the data set of density scan with 2.5MW (1MW 77GHz and 1.5MW 154GHz) heating. Density was scanned shot by shot. Approximately 2sec flat top was obtained. Perpendicular NB was injected for 20msec for every 400ms for T_i measurements using charge exchange spectroscopy (CXRS). This short pulse injection does not change T_i. Analysis timing was selected just before NB injection.

Density profile data from YAG laser Thomson scattering [18] is used for TASK3D power balance analysis. Figures 2 and 3 show profiles of n_e, T_e, T_i and χ_e, χ_i. As shown in Fig.2 (a) and Fig.3 (a), n_e profiles are hollowed. This is widely seen in NB heated plasma of LHD [16].

In the present analysis, charge exchange loss and convections loss are not included. This is because absolute neutral density profiles of hydrogen and deuterium were not measured. The charge exchange loss can reduce absorption power in plasma peripheral region. As described in the next section, global particle confinement is worse in D plasma. This indicates that neutral density is higher in D plasma than in H plasma for the same density. Higher neutral density in D plasma reduces absorption power in peripheral region and reduce χ_e, and χ_i compared with H plasma.

In low density case, as shown in Fig.2 (b), T_e and T_i profiles are almost identical. Ion heating is only due to the heat transfer from electron to ion. This heat transfer, which is equipartition heating, is shown by the following equation [19].

$$P_{ei} \propto \frac{Z_i^2 {n_e}^2}{m_i T_e^{3/2}} (T_e - T_i) \quad (2)$$

Here, Z_i is ion charge number and m_i is ion mass. Thus, for same density and same temperature difference between electron and ion, P_{ei} in H plasma is twice those in D plasma.

Similar density and almost identical T_e, T_i, as shown in Fig. 2(a) and (b), result in lower χ_i in D plasma as shown in Fig. 2(c). This is because P_{ei} is lower in D plasma than in H plasma. χ_e is almost identical in H and D plasma as shown in Fig.2 (c), this is partly because absorption energy to electron is not very different in H and D plasma.

In high density case, T_e is higher in D plasma, T_i is almost identical, n_e profiles are hollower and edge n_e is higher in D plasma. These differences of profiles result in higher stored energy and better energy confinement in D plasma than in H plasma. χ_i is lower in D plasma than in H plasma as well as low density case. In the low density case, χ_i is lower than χ_e in almost the entire region. On the other hand, in high density case, χ_i is higher than χ_e at $\rho > 0.5$.

Ion heating power increases in high density case compared with low density case. This can result in enhancement of transport due to the effects of power degradation. Power degradation is higher in H plasma due to the higher P_{ei} than in D plasma. Such effects are reported in ECRH L mode plasma of ASDEX-U [5].

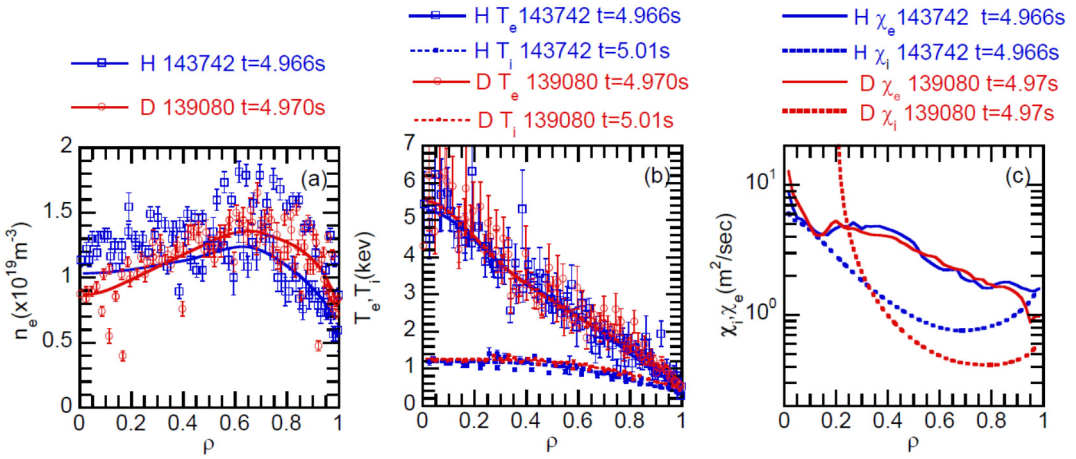

FIG.2 Low density case of (a) n_e,(b)T_e, T_i and (c) χ_e and χ_i profiles

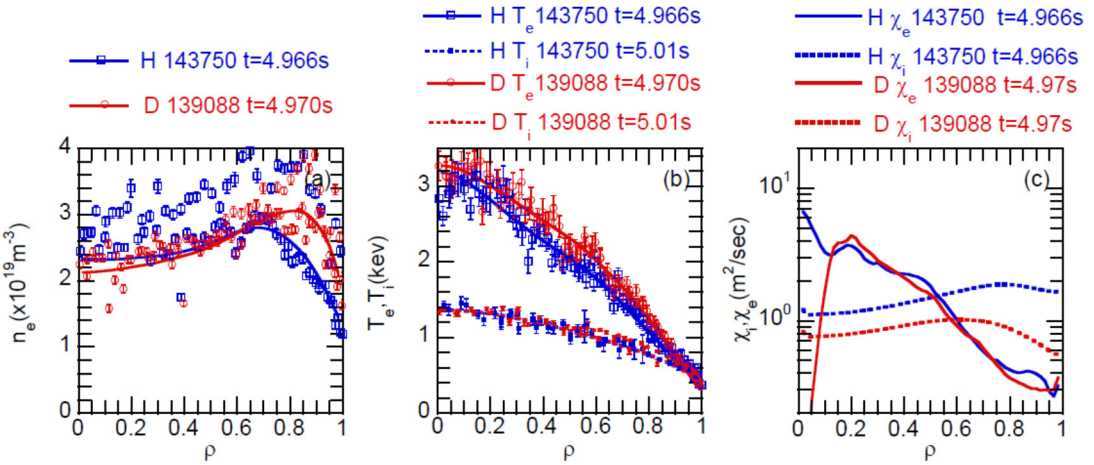

FIG.3 High density case of (a) n_e,(b) T_e, T_i and (c) χ_e and χ_i profiles

The neoclassical values of χ_e and χ_i were estimated for the shots in Fig.2 and Fig.3 by using GSRAKE code [20]. Figure 4 shows neoclassical estimation in low density case. In Fig.4 (a), radial electric field (Er) measured by using CXRS [21] are shown. The neoclassical

solutions are multiple at $\rho < 0.9$. The CXRS data show positive Er at $\rho = 0.7$~0.9 both in shot 143742 and 139080. The turbulence phase velocity measured by two dimensional phase contrast imaging (2D-PCI) [23,24] show ion diamagnetic propagation at $\rho = 0.5$ - 0.8. The ion diamagnetic propagation in laboratory frame suggests positive Er base on the assumption that the phase velocity is dominated by $E_r x B_t$ poloidal rotation. Thus, it is likely that Er at $\rho =$ 0.45~0.9 in 143742 and $\rho = 0.55$~0.9 in 139080 are positive and neoclassical root is electron root. Therefore, neoclassical Er, χ_e and χ_i in electron root are shown in Fig.4 (a) and (b). Both neoclassical χ_e and χ_i are almost the same in D plasma shot 143742 and in H plasma shot 139080. This indicates that there are no isotope effects of neoclassical transport in electron-root plasma.

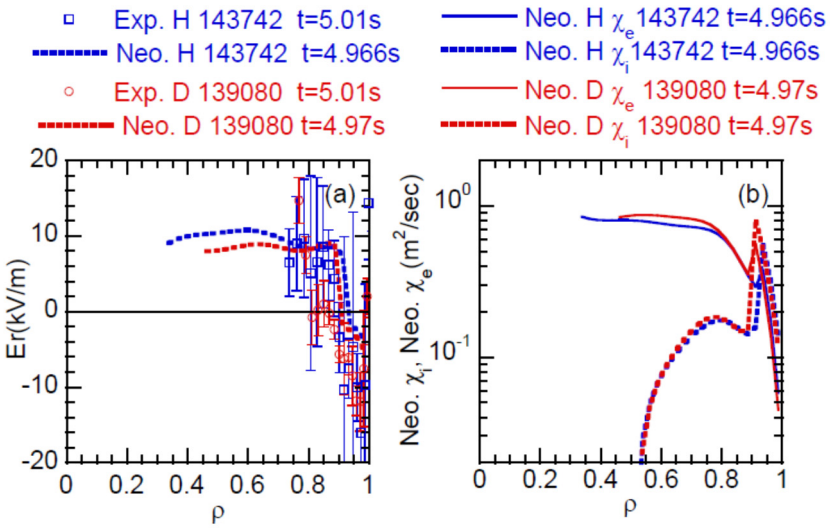

FIG.4 Low density case of neoclassical values (a) Er,(b) χ_e and χ_i
In (a), symbols indicate measured Er by using CXRS

Figure 5 shows neoclassical estimation in high density case. In H plasma shot 143750, neoclassical root is single ion root at $\rho > 0.35$. In D plasma shot 139088, neoclassical root is single ion root at $\rho > 0.4$. Neoclassical χ_e is almost identical, however, neoclassical χ_i is higher in D plasma at $\rho < 0.9$. This indicates that there is a negative isotope effects in neoclassical χ_i.

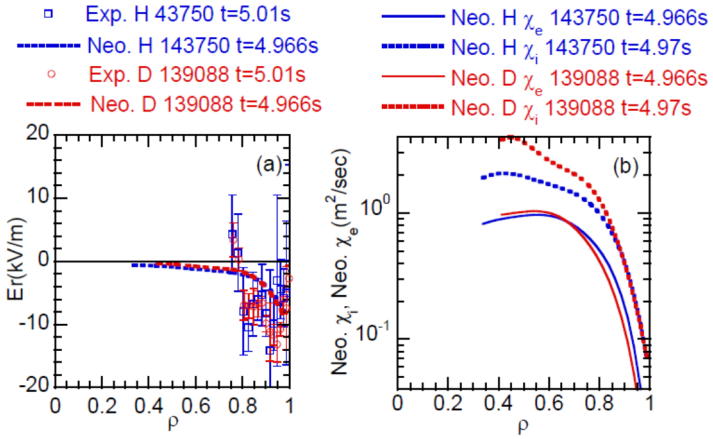

FIG.5 High density case of neoclassical values (a) Er,(b) χ_e and χ_i
In (a), symbols indicate measured Er by using CXRS

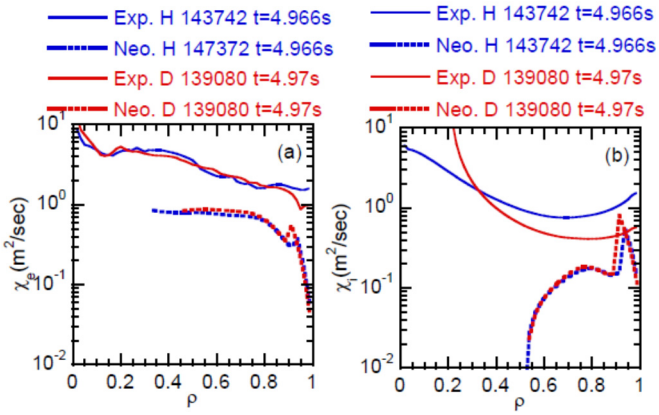

FIG.6 Comparison of experimental and neoclassical (a) χ_e and (b) χ_i in low density case

Figure 6 shows comparison between experimental and neoclassical χ_e and χ_i in low density case. As shown in Fig.6 (a), both neoclassical and experimental χ_e are almost identical. The neoclassical contribution in χ_e is less than 30%. The electron transport is dominated by anomalous process and there are no isotope effects. As shown in Fig.6 (b), neoclassical contribution in χ_i is also less than 30% at $\rho < 0.9$. Ion transport is dominated by anomalous process.

As shown in Fig.6 (b), the neoclassical χ_i is identical in H and D plasma. However, experimental χ_i is lower in D plasma than in H plasma. Thus, the anomalous contribution is lower in D plasma. Ion transport has an isotope effect.

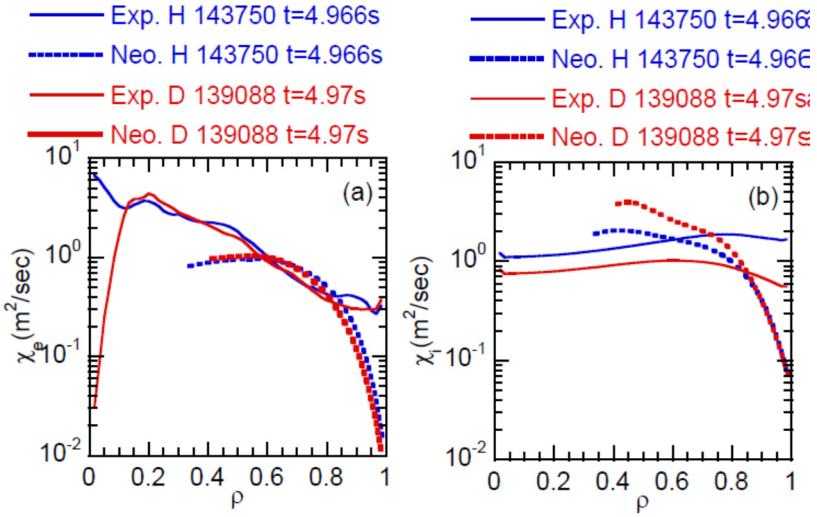

FIG.7 Comparison of experimental and neoclassical (a) χ_e and (b) χ_i in high density case

Figure 7 shows comparison between experimental and neoclassical χ_e *and* χ_i in high density case. As shown in Fig.7 (a), both neoclassical and experimental χ_e are almost identical as well as in the low density case. However, at $\rho < 0.85$ in H plasma and at $\rho < 0.8$ in D plasma, neoclassical χ_e becomes comparable with experimental χ_e. This indicates that core electron transport is accounted by the neoclassical transport. Only edge regions ($\rho > 0.85$ in H, and $\rho > 0.8$ in D plasma) are dominated by the anomalous process. The amount of anomalous contribution to χ_e in the edge region is almost comparable in H and D plasma indicating no isotope effects.

As shown in Fig.7 (b), neoclassical χ_i at $\rho < 0.6$ of H plasma exceeds experimental χ_i and neoclassical χ_i at $\rho < 0.85$ of D plasma exceeds experimental χ_i. These region should be

interpreted that transport is dominated by neoclassical process. Then, anomalous process play role at $\rho > 0.6$ in H plasma and $\rho > 0.85$ in D plasma. In H plasma, wider region is dominated by anomalous process then in D plasma.

Figure 8 shows collisionality dependence of χ_e and χ_i at three radial locations. χ_e decreases with increase of ν_h^*. χ_e both in H and D plasma show almost same value. On the other hand, χ_i in D plasma is lower at all locations. At $\rho = 0.5$ and 0.7, χ_i increases with increase of ν_h^*. This is an opposite tendency compared with χ_e. This tendency becomes moderate at $\rho = 0.9$. The difference of χ_e and χ_i become larger at more outer locations.

P_{ei} has strong proportionality to density (n_e^2) as shown in eq. (2), thus, in the dataset of density scan of Fig. 8, P_{ei} increase with collisionality. Thus, absorption power to the ion increases with collisionality. On the other hand, absorption power to electron decreases with increase of collisionality. The opposite collisionality dependence of absorption power to electron and ion results opposite collisionality dependence in χ_e and χ_i.

The present data set of power balance analysis showed there is no isotope effects in electron heat transport. There is an isotope effect in ion heat transport. χ_i is lower in D plasma than in H plasma.

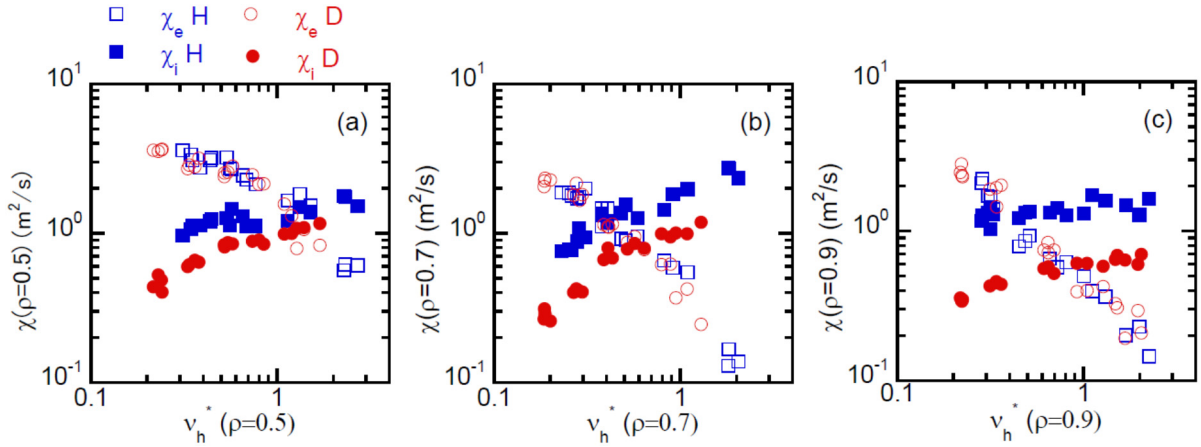

FIG.8 Collisionality dependence of χ_e and χ_i at (a) $\rho = 0.5$, (b) $\rho = 0.7$ and (c) $\rho = 0.9$

3. PARTICLE TRANSPORT

The global particle confinement time (τ_p) is estimated by the ratio between averaged density and the amount of particle source in steady state. Two different estimations were used for the particle source. One is by using neutral pressure gauge. Neutral pressure is an indication of edge particle source. Neutral pressure gauge is located in the main vacuum vessel. The other method is by using spectroscopic measurements. In the analysis method using spectroscopic data, particle source was estimated by the sum of the intensity of Hα, Dα and HeI lines. Then, τ_p was estimated for the data set of Fig.1 by using the following equations.

$$\tau_p = \frac{N_e}{S_e - {dN_e}/{dt}} \propto \frac{n_{e\,bar}}{Neutral\ Gas\ pressure} \propto \frac{n_{e\,bar}}{I_{H\alpha,D\alpha}+2HeI} \qquad (3)$$

τ_p from both methods are estimated in arbitrary unit. This is because absolute value of particle source is unknown and only relative change of particle source can be used for the comparison of τ_p. Figure 9 (a) and (b) shows collisionality dependence of τ_p by using two different methods. As shown in Fig.9 (a), τ_p from pressure gauge is clearly lower in D plasma. This indicates that neutral pressure is higher in D plasma than in H plasma at same line

averaged density. This is partly due to the higher recycling rate and partly due to the lower pumping speed in D plasma than in H plasma. The pumping speed of the cryo-sorption pump is inversely proportional to the square root of the molecular mass [24]. Thus, neutral pressure becomes higher in D plasma than in H plasma.

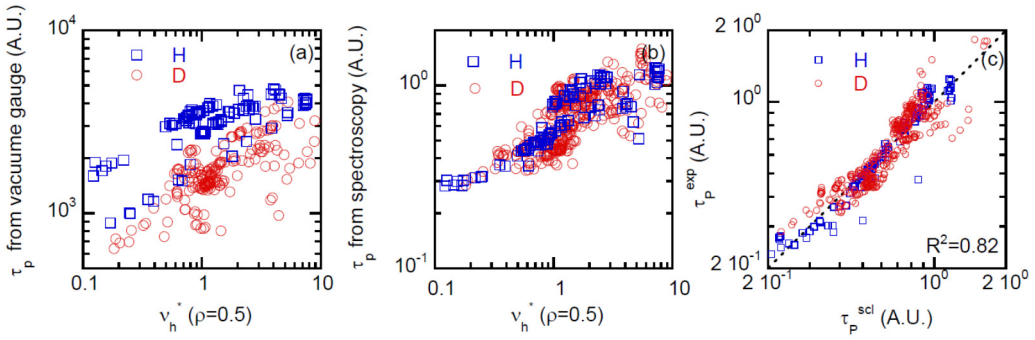

FIG. 9 τ_p of collisionality dependence (a) estimated from neutral pressure gauge, (b) estimated from spectroscopy, and (c) deduced scaling from spectroscopic τ_p.

τ_p from spectroscopy does not show clear difference as shown in Fig. 9 (b). However, the following scaling was obtained from regression analysis for the spectroscopic τ_p.

$$\tau_{P\,spec} \propto A^{-0.33\pm0.02}\bar{n}_e{}^{0.52\pm0.02}P_{abs}^{-0.69\pm0.02} \quad (4)$$

This is a significant contrast between larger $\tau_{E\,dia}$ and smaller $\tau_{p\ spec}$ in D plasma than in H plasma for the same $\bar{n}_e$ and P_{abs}.

Figure 10 (a)~(d) shows comparisons of n_e and T_e profiles in D and H plasma. Low and high density cases are shown. In Fig.10 (a) and (c), n_e profiles are from Abel inversion of multi-channel far infrared laser interferometer [25]. As shown in Fig. 10 (a)~(d), T_e profiles are almost identical in H and D plasma. However, n_e profiles are clearly different. Both in low and high density cases, n_e profiles in D plasma is hollower than H plasma. Also, edge peak positions of hollowed profiles, which are shown by the arrow, are more outward in D plasma than in H plasma. The particle source profile calculated by 3D Monte Carlo simulation code EIRENE shows that peaks of the particle source are at ρ =1.05 both in D and H plasma as shown in Fig. 10 (e). These peak positions are outer of edge peak of density profile. Also, the difference of neutral penetration is small in H and D plasma. Thus, the differences of n_e profiles are not due to the difference of the neutral penetration of hydrogen or deuterium.

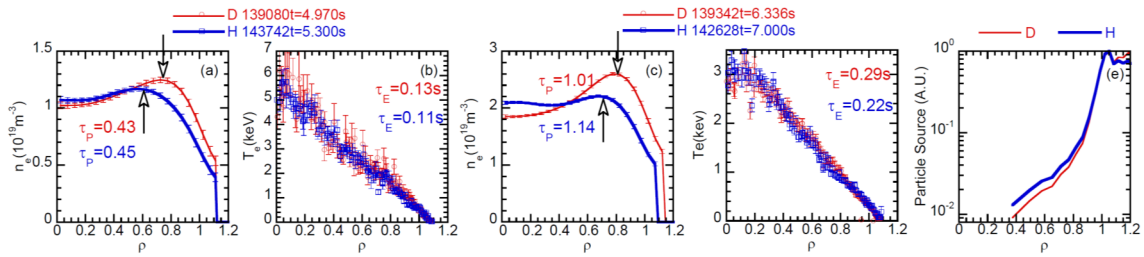

FIG.10 n_e and T_e profiles in (a),(b) low density, in (c),(d) high density and (e) Particle source of D and H plasma

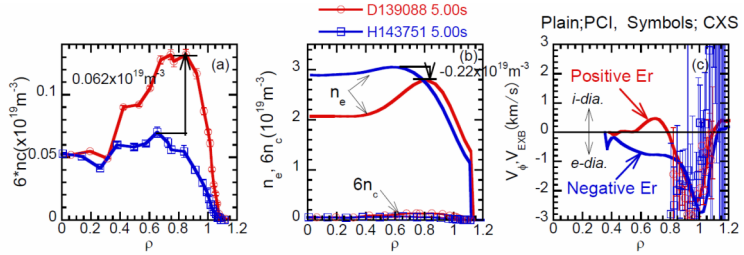

FIG.11 Comparison of (a) electron density profile ionized from C_6^+($6n_c$), (b) n_e and $6n_c$ and (c) turbulence phase velocity and E_rxB_t poloidal rotation velocity.

The effect of the impurity was investigated. The main impurity in core plasma of LHD is C_6^+. Main carbon source is carbon divertor plate. In D plasma, chemical and physical sputtering at divertor plate is enhanced. Then, influx of carbon is higher in D plasma than in H plasma [26]. Figure 11 (a) shows electron density from C_6^+ions ($6n_c$, where n_c is C_6^+ ion density from charge exchange spectroscopy). $6n_c$ is higher in D plasma due to the larger carbon influx. $6n_c$ profile is hollower in D plasma than in H plasma. However, difference of $6n_c$ profiles does not account for the difference of n_e profile. Because as shown in Fig.11 (b), edge peak n_e of D plasma is $0.22x10^{19}m^{-3}$ lower than edge peak n_e of H plasma, however, edge peak $6n_c$ density of D plasma is $0.062x10^{19}mm^{-3}$ higher than edge $6n_c$ density of H plasma as shown in Fig. 11(a). Thus, figures 10 and 11 indicate that hollower n_e profiles in D plasma are not due to the difference of impurity profile but rather are due to the difference of transport.

Figure 11 (c) shows turbulence phase velocity measured by two dimensional phase contrast imaging (2D-PCI) [22,23]. E_rxB_t poloidal rotation speed profiles measured by charge exchange spectroscopy [21] are over plotted. 2D-PCI measures poloidally dominated wavenumber, thus measured phase velocity indicates fluctuation phase velocity Doppler shifted by E_rxB_t rotation. Thus, the measured phase velocity can be an indicator of E_r.

As shown in Fig.11 (c), in D plasma, where $6n_c$ profile is extremely hollowed, phase velocity is ion diamagnetic propagation in laboratory frame. This suggests Er is positive. Neoclassical root is suggested to be electron root. On the other hand, in H plasma, where $6n_c$ profile is flat, the phase velocity is electron diamagnetic propagation. This suggests negative E_r. Neoclassical root is suggested to be ion root. One possible interpretation of hollower $6n_c$ profiles is due to the neoclassical effects of positive E_r, which transfers positively charged impurity ion outwardly.

Detail analysis of the particle transport were investigated by using density modulation experiments. Analysis is now underway.

4. TURBULENCE

Turbulence plays role on transport. Therefore, turbulence can play a role in isotope effects as well, when transport is dominated by the anomalous process. Gyrokinetic simulation predicts favorable isotope effects in the case trapped electron mode (TEM) govern the transport. The stabilization effects due to collision between the charged particle is higher in D plasma than H plasma [27]. This is direct isotope effects. In addition, the density profile can affects the linear stability both on TEM and ion temperature gradient mode (ITG). Lower negative gradient (-1/n dn/dr) reduces linear growth rate of TEM and ITG [28]. Thus, if there is a systematic difference of the density profile between H and D plasma, isotope effects can appear due to the difference of density profiles.

In the 19th (in the year of 2017) and the 20th (in the year of 2018-2019) LHD experimental campaign, turbulence were measured by two-dimensional phase contrast

imaging (2D-PCI) [22,23]. The measured frequency and wavenumber regions were 20 < 500 kHz and 0.1 < k < 0.8mm^{-1}. In the present dataset, $k_{perp}\rho_i$ is 0.1~1, where here k_{perp} is perpendicular wavenumber and ρ_i is ion Larmor. These wavenumber regimes are ITG and TEM ion scale turbulence.

Figure 12 shows the measured cross sectional view of 2D-PCI. The measurement quantity of 2D-PCI is line integrated fluctuation along the injected beam. With use of magnetic shear and strong asymmetry of turbulence wavenumber between perpendicular and parallel to the magnetic field, local measurements of the fluctuation becomes possible from the analysis of line integrated two dimensional turbulence picture [22,23]. The measured k is perpendicular to beam axis and magnetic field. Both radial and poloidal components contribute the signal. In most of the case, signal is dominated by poloidal components.

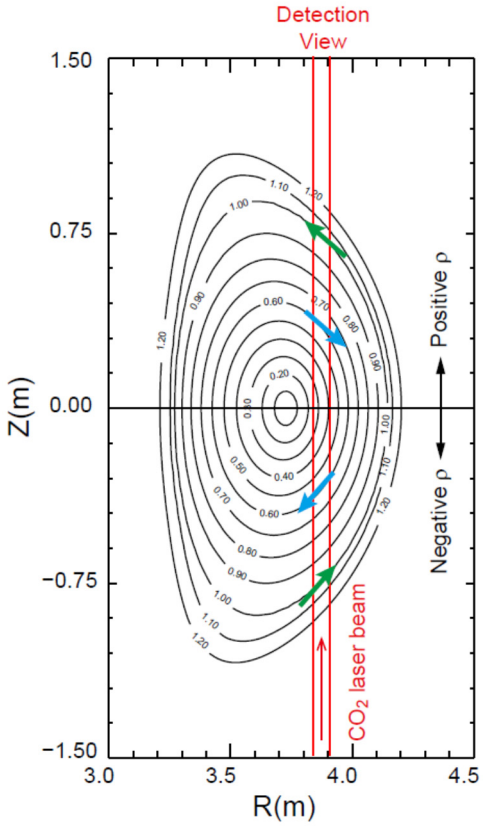

FIG. 12 Measured cross sectional view of 2D-PCI

The 2D-PCI is a kind of laser scattering technique using CO_2 laser. The signal intensity is a linear function of electron density turbulence amplitude. However, signal intensity is also affected by the laser power. Thus, it is essential to keep the laser stable in order not to change the signal due to the change of the laser power. In particular, this is important to compare the signal of a different experimental day. In the 20th campaign (2018-2019), the CO_2 laser was carefully tuned and stabilized. Also, change of the laser power and wavelength were monitored. In the dataset analyzed in this paper, the difference of power at different experimental day are maximum 3% and difference of the wavelength is maximum 0.1%. The small difference of the power were also calibrated for the estimation of turbulence level. Thus, precise comparison of fluctuation amplitude became possible and systematic comparison of the ion scale turbulence was carried out.

Figure 13 shows time trace of H (shot 15249, 152264, 152270) and D (shot 147826, 147824, 147829). The heating is 2MW 154GHz second harmonic on axis heating. One path deposition is more than 88% of injection power. In the dataset, there is 5~10% He contamination, but other portions are pure H and D ions. The configuration was Rax=3.6m, Bt=2.75T.

As shown in Fig. 13 (a-1), (b-1) and (c-1), the line averaged density was adjusted both for H and D plasma. Figure 13 (a-2), (b-2), (c-2), (a-3), (b-3), (c-3) show line integrated fluctuation signals for 20~200kHz and 200-500kHz. The 20~200kHz and 200~500kHz are approximately core and edge fluctuation, respectively. Fluctuation amplitude of 20~200kHz is higher in D plasma than in H plasma at low and middle density, but lower in D plasma than in H plasma at high density. On the other hand, fluctuation amplitude of 200~500kHz is lower in D plasma at all density regime and the difference becomes larger at higher density. As shown in Fig.13 (a-4), (b-4) and (c-4), central T_e is almost identical at low density both in H and D plasma and central T_e becomes higher in D plasma than in H plasma at higher density. On the other hand, central T_i is almost identical both in H and D plasma. Figure 13 indicates that turbulence characteristics are different for identical density and heating power in H and D plasma. These are turbulence isotope effects.

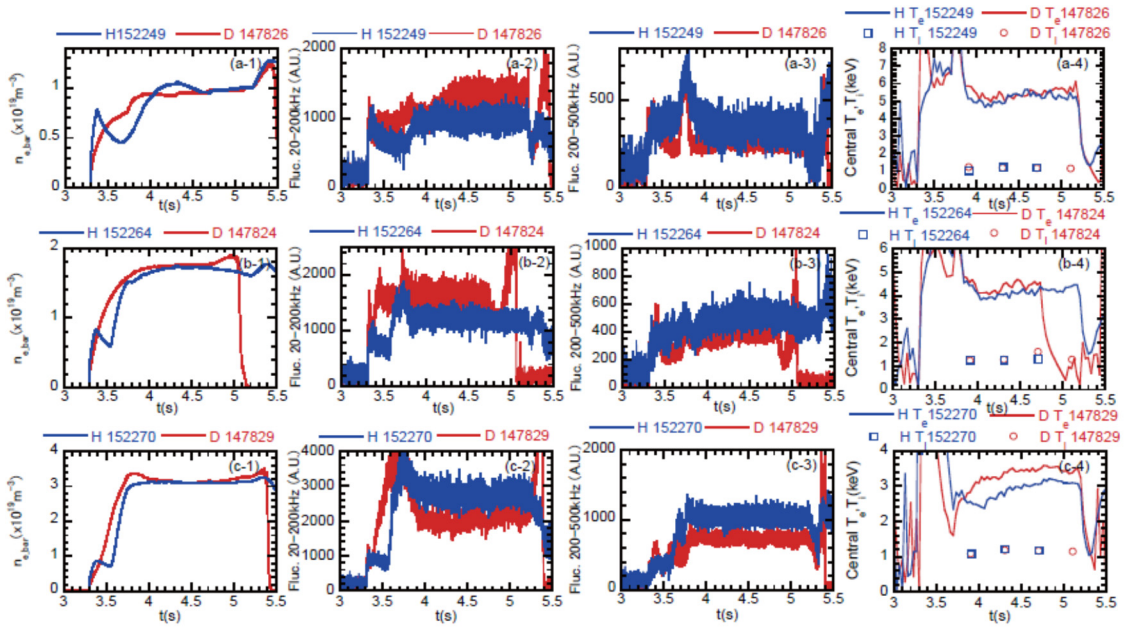

FIG.13 Comparison of time trace in (a) low, (b) middle and (c) high density. (a-1),(b-1),(c-1); line averaged density, (a-2),(b-2),(c-2); line integrated fluctuation amplitude for 20-200kHz by 2D-PCI, (a-3),(b-3),(c-3); line integrated fluctuation amplitude for 200-500kHz by 2D-PCI, (a-4),(b-4),(c-4);central electron and ion temperature at ρ=0~0.2 measured by Thomson scattering and CXRS

In Figs. 14 - 16, n_e, T_e, T_i and fluctuation spatial profiles are shown for low, middle and high density. Profiles are 0.5sec accumulated in order to obtain good quality of profiles. The turbulence spatial structures are different at three density regimes.

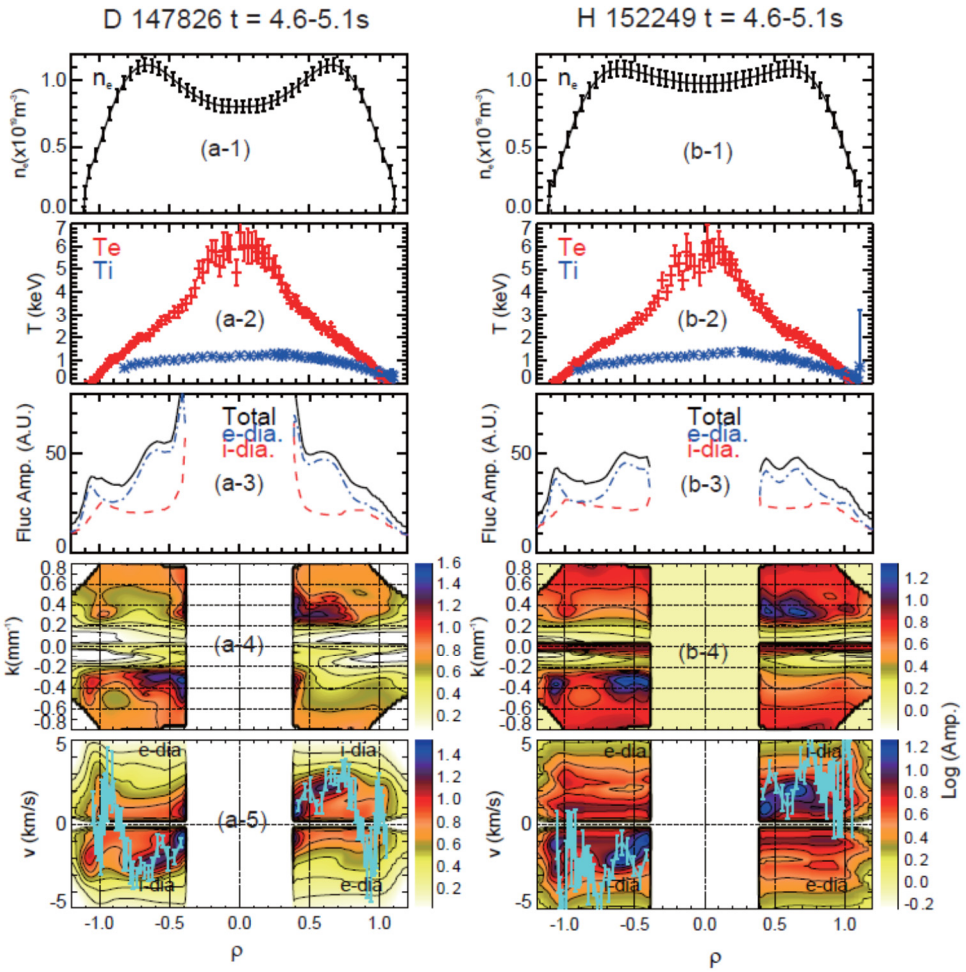

FIG. 14 Profiles in D plasma (a-1)~(a-5) and H plasma (b-1)~(b-5) of low density plasmas. (a-1),(b-1) n_e, (a-2),(b-2) T_e and T_i profiles, (a-3),(c-3) electron density fluctuation amplitude, (a-4), (d-4) contour plot of fluctuation amplitude k spectrum and (a-5), (b-5) contour plot of fluctuation amplitude phase velocity in laboratory frame. In (a-5) and (b-5), blue lines indicate $E_r x B_t$ poloidal rotation velocities measured by CXRS.

As shown in Fig. 14, in low density regime, dominant turbulence amplitude exists at $\rho < 0.8$ both in D and H plasma. Figure 14 (a-3)~(a-5), (b-3)~(b-5) suggest that turbulence expand $\rho < 0.4$, where 2D-PCI is not accessible. The turbulence at $\rho = 0.4$~0.8 propagates toward the ion diamagnetic direction in laboratory frame. The small peak is seen at $\rho = 1.0$, which propagates toward the ion diamagnetic direction in laboratory frame as well. The spatial structure is similar, however, fluctuation amplitude is larger in D plasma than in H plasma. As shown in Fig.14 (a-5),(b-5), phase velocities of the turbulence follow $E_r x B_t$ poloidal rotation velocity (V_{EXB}) measured by CXRS both in D and H plasma.

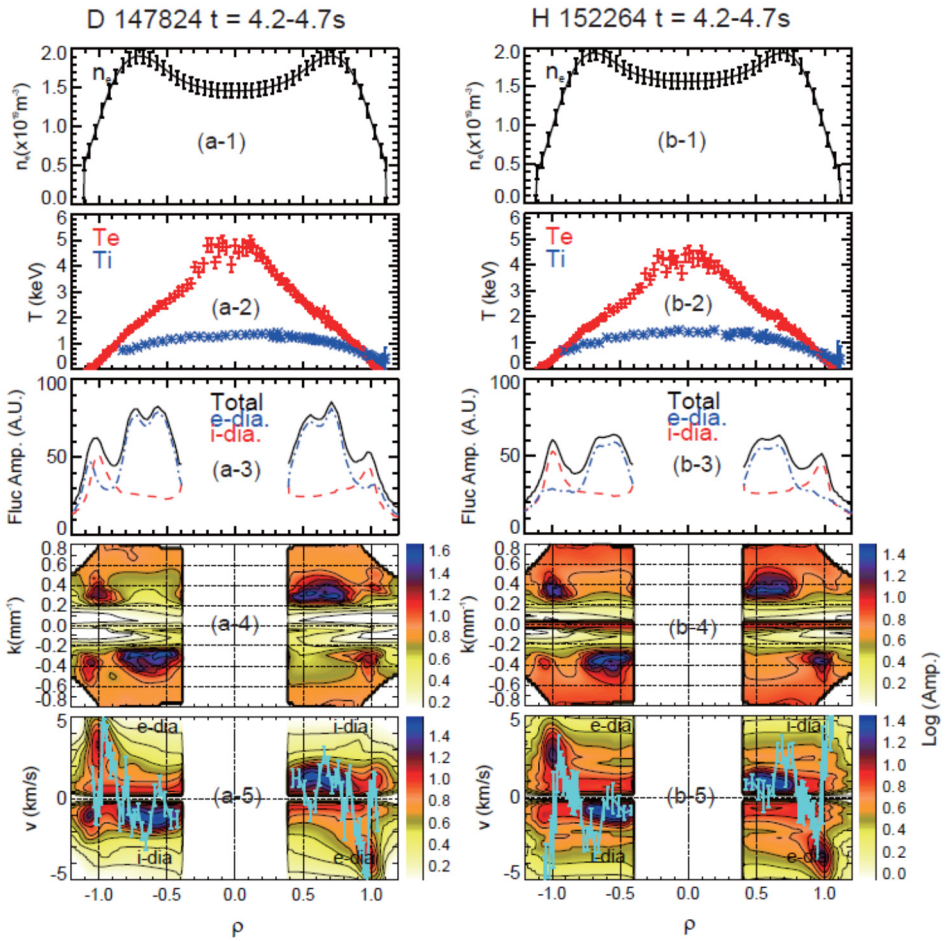

FIG. 15 Profiles in D plasma (a-1)~(a-5) and H plasma (b-1)~(b-5) of middle density plasmas. (a-1),(b-1) n_e, (a-2),(b-2) T_e and T_i profiles, (a-3),(c-3) electron density fluctuation amplitude, (a-4), (d-4) contour plot of fluctuation amplitude k spectrum and (a-5), (b-5) contour plot of fluctuation amplitude phase velocity in laboratory frame. In (a-5) and (b-5), blue lines indicate $E_r xB_t$ poloidal rotation velocities measured by CXRS.

As shown in Fig.15, in the middle density, the peaks of the fluctuation amplitude are ρ = 0.6 ~ 0.8 both in D and H plasma. These components propagate toward the ion diamagnetic direction in laboratory frame. The peak at ρ =1.0 becomes clearer compared with low density case. In D plasma, as shown in Fig.15 (a-5), there are two peaks at ρ =1.0 and 1.1. The former and latter propagate toward the electron and ion diamagnetic direction in laboratory frame respectively. As shown in Fig.15 (a-5),(b-5), the V_{EXB} also shows the changes the same way. Turbulence phase velocities follows V_{EXB} both in D and H plasma. The spatial structure is similar in D and H plasma. However, fluctuation amplitude is clearly higher in D plasma than in H plasma.

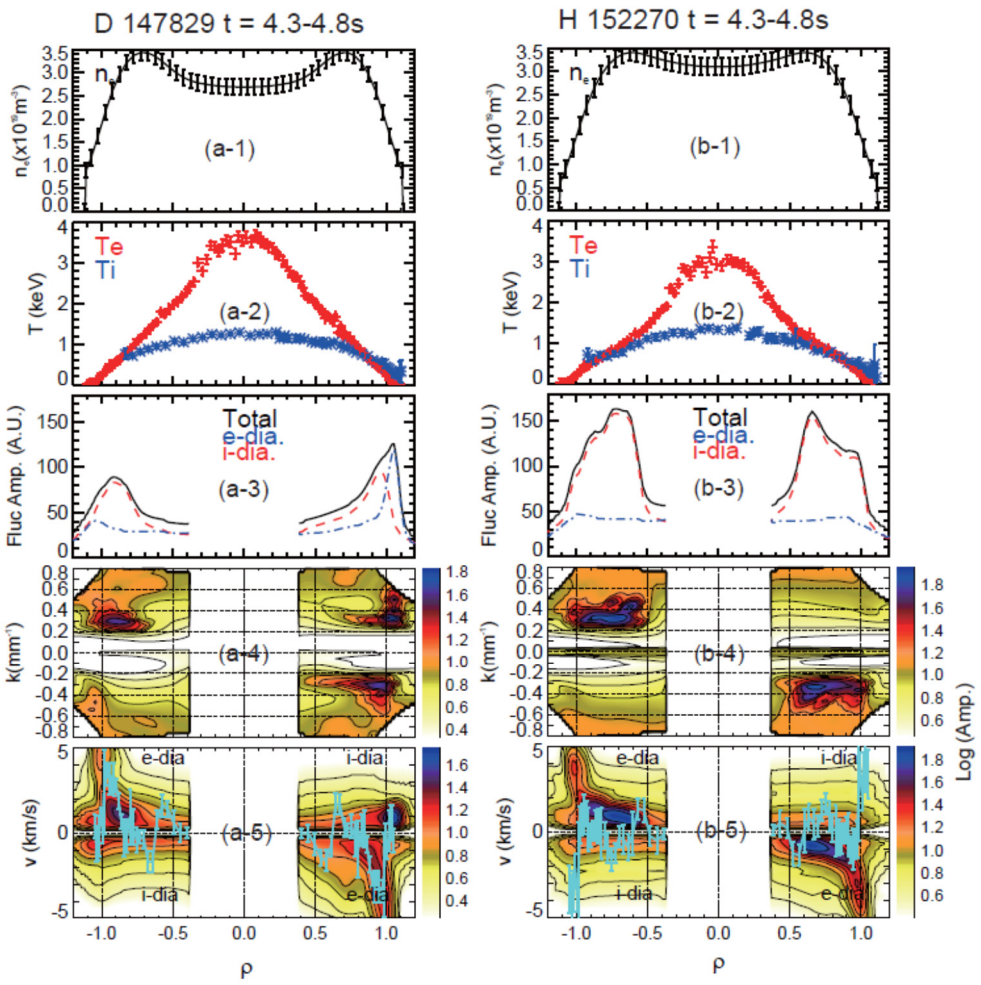

FIG. 16 Profiles in D plasma (a-1)~(a-5) and H plasma (b-1)~(b-5) of high density plasmas. (a-1),(b-1) n_e, (a-2),(b-2) T_e and T_i profiles, (a-3),(c-3) electron density fluctuation amplitude, (a-4), (d-4) contour plot of fluctuation amplitude k spectrum and (a-5), (b-5) contour plot of fluctuation amplitude phase velocity in laboratory frame. In (a-5) and (b-5), blue lines indicate $E_r x B_t$ poloidal rotation velocities measured by CXRS.

As shown in Fig. 16, in the high density plasma, the density turbulence profiles are clearly different in D and H plasma. As shown in Fig. 16 (a-3), (b-3), turbulence amplitude is clearly smaller in D plasma than in H plasma. In D plasma, the peak of the turbulence is at ρ =1.0. On the other hand, in H plasma, the peak of the turbulence is around ρ = 0.7. In addition, in H plasma, turbulence exists wider region compared with D plasma. In low and middle density, the turbulence spatial structures are similar in H and D plasma, however, turbulence amplitude is larger in D plasma than in H plasma. This indicates that unstable region is the same in D and H plasma, but saturation level is different. On the other hand, in high density, different spatial structures are also clearly different in addition to turbulence amplitudes. These indicate that unstable spatial region is different in H and D plasma. In D plasma, turbulence phase velocities follow V_{EXB} as shown in Fig. 16 (a-5). On the other hand, in H plasma, turbulence phase velocity is further toward the electron diamagnetic direction compared with V_{EXB} at ρ ~ 0.7 as shown in Fig.16 (b-5). This observation suggests that the turbulence propagates toward the electron diamagnetic direction in plasma frame at ρ ~ 0.7 in H plasma.

Figure 17 shows collisionality dependence of turbulence level and normalized gradients. Turbulence level was turbulence amplitude normalized by electron density. The turbulence level was averaged for core (ρ = 0.5 ~ 0.8) and edge (ρ = 0 8~1.1). This is because turbulence

structure is different at core (ρ = 0.5 ~ 0.8) and edge (ρ = 0 8~1.1) as shown in Figs.14 ~ 16. The collisionality and normalized gradient was averaged for core (ρ = 0.5 ~ 0.8) and edge (ρ = 0 8~1.0). The n_e profiles are fitted by 8^{th} order polynomial function and ,T_e and T_i profiles are fitted by the 6^{th} order polynomial function for ρ = 0 ~ 1.0. This is because fitting becomes inappropriate including the data at ρ > 1.0 due to the scattering of the data. On the other hand, the turbulence has a large components at ρ >1.0, thus, the edge turbulence peak was estimated at ρ = 0 8~1.1. Also, turbulence level was estimated for upper side of equatorial plane and lower side of equatorial plane. Both side shows similar dependence. However, there are asymmetry between upper and lower side in some cases.

As shown in Fig. 17 (a), the core turbulence peak has a V shape dependence on the ν_h^*. The turbulence level decreases with ν_h^* up to ν_h^*=4, then the turbulence level increases with ν_h^* at $\nu_h^* > 4$. At $\nu_h^* < 2$, the turbulence level is lower in H plasma than in D plasma. Then, at $\nu_h^* > 4$, turbulence level is higher in H plasma than in D plasma. As shown in Fig. 17 (b), normalized T_e and T_i gradients are almost constant at $\nu_h^* < 2$. Only the normalized density gradient is reducing. Thus, the normalized density gradient is likely to be the driving term. However, it should be noted that normalized density gradient is lower in D plasma at $\nu_h^* < 2$, although turbulence level is higher in D plasma. The magnitude relationship of turbulence level between H and D plasma exchanges at ν_h^* ~3. This observation qualitatively agree with theoretical expectation, where TEM has stronger collisionality stabilization effects in D plasma than in H plasma [28].

On the other hand, at $5 < \nu_h^* < 10$, the all normalized gradient increases with increase of ν_h^* both in H and D plasma. Experimentally, the driving term is not clear in this regime.

In ATF, of which magnetic configuration is similar to LHD, it was reported that measured core turbulence was dissipative trapped electron mode (DTEM) [29]. The linear growth rate of DTEM increase with increase of collisionality. The increase of the turbulence level with increase of the collisionality were reported. Qualitatively, the observation in ATF is similar to the results at $\nu_h^* > 4$ in LHD. However, more detail analysis using gyrokinetic simulation is necessary to identify the turbulence.

Figure 17 (c) and (d) show ν_h^* dependence of edge turbulence level and normalized gradient. Clear exchange of the magnitude relationship of turbulence level between H and D plasma are not observed. The turbulence level is comparable at $\nu_h^* < 2$ and becomes lower in D plasma at $\nu_h^* > 2$. The turbulence level is the lowest at ν_h^* = 2~5 in H plasma and the lowest at ν_h^* = 2 ~ 10 in D plasma. The normalized gradient does not change clearly. As well as core region, at higher ν_h^*, the turbulence level becomes clearly lower in D plasma. But ν_h^* dependence and normalized gradient dependence is not as clear as core turbulence. More detail argument is necessary.

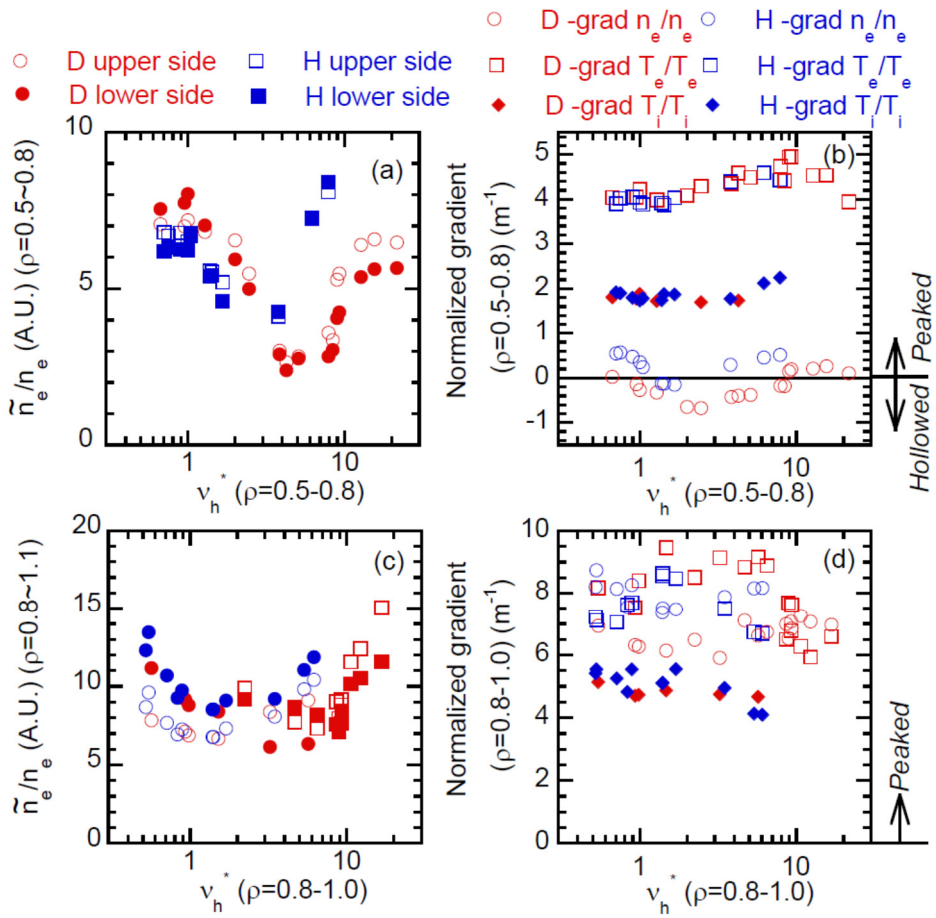

FIG. 17 Collisionality dependence of (a) core turbulence level, (b) core normalized gradient, (c) edge fluctuation level and (d) edge normalized gradient. Some data of D plasma lacks T_i profile.

5. DISCUSSION AND SUMMARY

Extensive investigation of isotope effects were performed for ECRH plasma of LHD. Unlike tokamak, ELM and MHD activity such as sawteething do not appear and do not disturb plasma, thus, precise comparisons are possible. The data at analysis timing was free from beam heating effects. Thus, present data set is purely external electron heating plasma. Global energy confinement time is 16% better in D plasma than in H plasma. Power balance analysis for density scan dataset with constant injection power showed comparable χ_e and reduced χ_i in D plasma. Ref.1 and Ref.2 report that injection direction of tangential ECRH plays a role on the isotope effects. This suggests that change of iota profile affects isotope effects. However, in the dataset analysed in this paper, tangential ECRH were almost balanced, thus, effects of tangential injection of ECRH do not affect isotope effects.

Local power balance analyses were performed. χ_i increase with ν_h^* and χ_e decrease with ν_h^*. The opposite ν_h^* dependence is likely to be the effects of equipartition heating power. The equipartition heating power increase with increase of ν_h^*. Then, increase of ν_h^* results in decrease of electron heating power, then, χ_e reduces. On the other hand, increase of ν_h^* results in increase of ion heating power, then, χ_i increases possibly with power degradation effects. Comparable χ_e and reduced χ_i in D plasma rather than in H plasma were found. Experimentally, isotope effects was seen only in ion energy channel in the present dataset of power balance analyses. Thus, the improved confinement of global energy confinement is likely to be due the improvement of ion energy confinement.

Neoclassical estimations were performed in low and high density case. In low density case, neoclassical root was electron root. There are no isotope effects in neoclassical χ_e and χ_i, while experimental χ_i is lower in D plasma than in H plasma. This indicates anomalous contribution of χ_i is lower in D plasma. In high density, neoclassical root was ion root, there is no isotope effects in neoclassical χ_e, but isotope effects appears in χ_i. Neoclassical χ_i is higher in D plasma than in H plasma, although experimental χ_i is lower in D plasma than in H plasma. Thus, anomalous contribution of χ_i is lower in D plasma.

Global particle confinement is enhanced in D plasma. This is confirmed by τ_p from neutral pressure gauge and τ_p from spectroscopy. Density profiles are more hollowed in D plasma than in H plasma. This is not due to the difference of neutral penetration or impurity sources rather due to the difference of the transport.

Ion scale turbulence was measured by 2D-PCI. Precise comparison was performed from the monitoring of the probe laser. The isotope effects were found in ion scale turbulence. In core region ($\rho = 0.5 - 0.8$), turbulence level is lower in H plasma at $\nu_h^* < 2$ and turbulence level is higher in D plasma at $\nu_h^* > 2$. The core turbulence level decreases with increase of ν_h^* at $\nu_h^* < 4$. The driving term of the turbulence at $\nu_h^* < 4$ is likely to be the normalized density gradient. The exchange of the magnitude relationship qualitatively agree with gyrokinetic prediction of TEM [28]. At $\nu_h^* > 4$, the core turbulence level increases with ν_h^* both in H and D plasma. Driving term is not clear at this collisionality region.

In edge region ($\rho = 0.8$-1.1), the turbulence level is comparable at $\nu_h^* < 2$ in H and D plasma and the turbulence level is lower in D plasma than in H plasma. Driving term is not clear since normalized gradient was almost constant at the present dataset. Isotope effects of the turbulence are different in spatial region and collisionality region. In next step, comparison with gyrokinetic simulation is necessary for the further understanding.

Isotope effects of ECRH plasma in LHD are different in ion energy transport electron energy transport and particle transport. Recent analysis regarding NB heating plasma showed that τ_E does not show ion mass dependence [30]. This is in clear contrast to the result of ECRH plasma described in this paper. This suggests isotope effects vary on heating channel as well. Also, comparison with helium plasma will also provide additional knowledge for ion mass and charge number effects. This is performed for H and He plasma with NB heating [31]. Experiments in He plasma with ECRH are expected.

ACKNOWLEDGMENTS

This work is supported by NIFS grants NIFS17ULHH013, NIFS18ULHH013, NIFS18KLER045, NIFS18KLPH032, NIFS18KUHL083, NIFS19KLPH038 and JSPS grant 16H04620.

REFERENCES

[1] ITER Physics Basis Expert Groups on Confinement and Transport and Confinement Modelling and Database and ITER Physics Basis Editors 1999 Nucl. Fusion 39 2175
[2] YAMADA, H. et al, Nucl. Fusion, **45**, (2005)1684
[3] MAGGI, C.F., et al, Plasma Phys. Control. Fusion **60** (2018) 014045
[4] URANO, H. et al 2012 Phys. Rev. Lett. 109 125001
[5] SCHNEIDER, P.A. et al, Nucl. Fusion **57** (2017) 066003
[6] YAMADA, H., et al, Fusion Sci, Tech. **44** (2004) 82
[7] TANAKA, K., et al, Plasma Phys. Control. Fusion **58** (2016) 055011
[8] OHTANI Y., et al, Journal of the Physical Society of Japan **86**, (2017) 064501

[9] TAKEIRI, Y., et al, IEEE Transactions on Plasma Science **46**, (2018) 2348
[10] TAKAHASHI, H., et al, Nucl. Fusion **58** (2018) 106028
[11] WARMER, F., et al, Nucl. Fusion **58** (2018)106025
[12] IGAMI, H., et al, EPJ Web of Conferences **203**, 02001 (2019) https://doi.org/10.1051/epjconf/201920302001
[13] TSUJIMURA, T., et al, Nucl. Fusion 55 (2015) 123019
[14] MURAKAMI, S., Nucl. Fusion **42**, (2002) L19–L2
[15] YOKOYAMA, M., et al, J. Plasma Fusion Res. **81**, (2005) 83
[16] TANAKA, K., et al, Fusion Sci. Tech. **58**, (2010), 70
[17] YOKOYAMA, M. et al, "Extended Capability of the Integrated Transport Analysis Suite, TASK3D-a, for LHD Experiment, and its Impacts on Facilitating Stellarator-Heliotron Research"[FIP/P7-35], paper presented at 25th IAEA Int. Conf. on Fusion Energy, Saint Petersburg, 2014
[18] YAMADA, I., et al, Fusion Sci. Tech. **58**, (2010) 345
[19] WESSON J.A., 1997 Tokamaks 2nd edition (Oxford: Clarendon)
[20] BEIDLER, C. D., and HITOCHON, W. N. G., Plasma Phys. Control. Fusion, 36, (1994), 317
[21] YOSHINUMA, M., et al, Fusion Sci. Tech. **58**, (2010) 37
[22] TANAKA, K., et al, Rev. Sci. Instrum. **79**, (2008), 10E702
[23] MICHAEL, C., et al, Rev. Sci. Instrum. **86**, (2015), 093503
[24] MOTOJIMA, G., et al, Nucl. Fusion, **59**, (2019), 086022
[25] TANAKA, K., et al, Plasma Fusion Res **3**, (2008) 050
[26] MASUZAKI, S., presented at 21st Int. Stellarator–Heliotron Workshop (Kyoto, Japan 2–6 October 2017)
[27] NAKATA, M., et al, Phys. Rev. Lett. **118**, (2017), 165002
[28] NAKATA, M., et al, Plasma Phys. Ctrl. Fusion **61** (2019) 014016
[29] SHATS, M. G., et al, Phys. Plasmas **2**, (1995), 398
[30] YAMADA, H., et al, "Characterization of Isotope Effect on Confinement of Dimensionally Similar NBI-Heated Plasmas in LHD ". Preprint : 2018 IAEA Fusion Energy Conference, Gandhinagar [EX/P3-5]
[31] TANAKA, K., et al, Nucl. Fusion **57** (2017) 116005